Long-lasting effect of mercury contamination in the soil microbiome and its co-selection of antibiotic resistance

Khandaker Rayhan Mahbub* School of Life Sciences, University of Technology Sydney, Ultimo, NSW 2007, Australia; Current Address: South Australian Research and Development Institute, Urrbrae, SA 5064, Australia.

William L King School of Life Sciences, University of Technology Sydney, Ultimo, NSW 2007, Australia; Climate Change Cluster, University of Technology Sydney, Ultimo, NSW 2007, Australia

Nachshon Siboni Climate Change Cluster, University of Technology Sydney, Ultimo, NSW 2007, Australia

Viet Khue Nguyen School of Life Sciences, University of Technology Sydney, Ultimo, NSW 2007, Australia; Climate Change Cluster, University of Technology Sydney, Ultimo, NSW 2007, Australia

Mohammad Mahmudur Rahman Global Centre for Environmental Remediation, The University of Newcastle, Callaghan, NSW 2308, Australia

Mallavarapu Megharaj Global Centre for Environmental Remediation, The University of Newcastle, Callaghan, NSW 2308, Australia

Justin R Seymour Climate Change Cluster, University of Technology Sydney, Ultimo, NSW 2007, Australia

Ashley E. Franks Department of Physiology, Anatomy and Microbiology, La Trobe University, Bundoora, VIC 3086, Australia; Centre for Future Landscapes, La Trobe University, Bundoora, VIC 3086, Australia

Maurizio Labbate* School of Life Sciences, University of Technology Sydney, Ultimo, NSW 2007, Australia

***Author for correspondence**

Khandaker Rayhan Mahbub

School of Life Sciences, University of Technology Sydney, NSW 2007, Australia

Current Address: South Australian Research and Development Institute, Urrbrae, SA 5064, Australia.

Email: krmjissan@gmail.com; Khandaker.mahbub@sa.gov.au; phone: +61404022697

Maurizio Labbate

School of Life Sciences, University of Technology Sydney, NSW 2007, Australia

Email: Maurizio.Labbate@uts.edu.au; phone: +610414860609

Highlights

- Mercury can co-select for antibiotic resistance genes in soil.
- Mercury is naturally attenuated in soil following long-term ageing.
- Natural attenuation is not sufficient to restore health of mercury-contaminated soil.
- ARG co-selection is strongly correlated with microbiota shift and soil chemistry.

Abstract

Antibiotic resistance genes (ARGs) in the environment are an exposure risk to humans and animals and is emerging as a global public health concern. In this study, mercury (Hg) driven co-selection of ARGs was investigated under controlled conditions in two Australian non-agricultural soils with differing pH. Soils were spiked with increasing concentrations of inorganic Hg and left to age for 5 years. Both soils contained ARGs conferring resistance to tetracycline (*tetA, tetB*), sulphonamides (*sul1*), trimethoprim (*dfrA1*) and the ARG indicator class 1 integron-integrase gene, *intI1,* as measured by qPCR. The last resort antibiotic vancomycin resistance gene, *vanB* and quinolone resistance gene, *qnrS* were not detected. Hg driven co-selection of several ARGs namely *intI1*, *tetA* and *tetB* were observed in the alkaline soil within the tested Hg concentrations. No co-selection of the experimental ARGs was observed in the neutral pH soil. 16S rRNA sequencing revealed proliferation of *Proteobacteria* and *Bacteriodetes* in Hg contaminated neutral and alkaline soils respectively. Multivariate analyses revealed a strong effect of Hg, soil pH and organic carbon content on the co-selection of ARGs in the experimental soils. Additionally, although aging caused a significant reduction in Hg content, agriculturally important bacterial phyla such as *Nitrospirae* did not regrow in the contaminated soils. The results suggest that mercury can drive co-selection of ARGs in contaminated non-agricultural soils over five years of aging which is linked to soil microbiota shift and metal chemistry in the soil.

Mercury can drive co-selection of antibiotic resistance genes in non-agricultural soils. The co-selection process is linked with soil properties, mercury content and soil microbiota shift.

Key words: soil; metal; antimicrobial resistance; inorganic mercury; ARGs.

1. Introduction

Human overuse of therapeutic antibiotics and other antimicrobial substances and their subsequent dispersal into the environment facilitates the selection or co-selection for antibiotic resistance genes (ARGs). ARGs are ubiquitous in environments contaminated with human and animal waste (Singer and others 2016). Co-selection of antibiotic and metal resistance occurs when resistance for both is conferred by the product of the same gene(s)

(e.g. efflux pump), or when the metal and antibiotic resistance determinants are harboured on the same mobile genetic element (MGE, a genetic material that can mobilize, e.g. a plasmid) or when the regulation of the resistance genes are transcriptionally linked (e.g. co-regulation of two different efflux pumps) (Baker-Austin and others 2006). Evidence supporting metal driven co-selection of ARGs in different environments is mounting, however, most research has principally been performed in aquatic environments rather than soils (Gorovtsov and others 2018).

In terrestrial environments, there has been a focus on agricultural soils with added animal manure and biosolids containing ARGs, elevated metal concentrations and antibiotics (Gorovtsov and others 2018; Zhou and others 2017). In non-agricultural soils, there is limited evidence of metal-driven co-selection of ARGs (Ji and others 2012; Knapp and others 2011). The co-selection of long-lasting metals with ARGs is important as it allows soils to act as ARG reservoirs and helps facilitate the movement of ARGs across indigenous bacterial communities through lateral gene transfer (LGT) processes. In the context of antibiotic resistance, mobile genetic elements (MGEs) have greatly facilitated the recruitment of novel ARGs from diverse environmental sources into bacterial pathogens and, human and animal commensal bacteria (Gillings and others 2008; Vikesland and others 2017).

Mercury (Hg) is a highly toxic metal, which has no known biological function and causes disruption in environmental health even at very low concentrations (Mahbub and others 2017a). Hence, Hg contamination and its impact on different components of an ecosystem has attracted significant attention from the international scientific community. Among various Hg species in soil, inorganic Hg is toxic for humans, disrupts soil biota at all trophic levels and can be bio-magnified in the food web. Additionally, under anaerobic conditions in water-logged soils or sediments, Hg is as a substrate for bacterial methylation producing methyl mercury, a neurotoxin (Bjørklund and others 2017; Lohren and others 2015; Mahbub and others 2017a).

Soil is a heterogeneous matrix where Hg stably complexes with chlorides, sulphides or organic materials. Various soil factors, predominantly pH, organic carbon content, ions and clay material are instrumental for determining Hg's fate and bioavailability (de Vries and others 2007). Due to its strong association with soil particles and organic materials, Hg is poorly detectable in soil solutions under natural conditions. Even in minute bioavailable amounts (less than approximately 0.001% of its total content), Hg can affect soil microbial

activities and community compositions (Frossard and others 2018; Mahbub and others 2017c; Müller and others 2001). The suggested safe limits or ecological investigation limits (EILs) for inorganic Hg in soil are as low as 1 mg/kg in Australia, however, recent studies suggest that inorganic Hg can exert toxicity at lower than 1 mg/kg concentration on soil dwelling microbes, plants and invertebrates (de Vries and others 2007; Mahbub and others 2018). In addition to the detrimental impact of Hg on human and environmental health, recent data have shown that Hg co-selects for ARGs in the environment (Gorovtsov and others 2018; Wardwell and others 2009). Such co-selection is attributed to the co-occurrence of Hg resistance genes and ARGs on various MGEs (Mathema and others 2011; Wireman and others 1997). Generally, Hg resistant bacteria contain a well-studied genetic trait called the *mer* operon that encodes proteins for transport (*merT, merP, merF*), and detoxification (*merA, merB*) of toxic inorganic Hg to a less toxic and less soluble metallic Hg which is volatilized from bacterial cells (Dash and Das 2012).

Proliferation of metal resistant bacterial taxa such as *Proteobacteria* and *Verrucoicrobia* in Hg contaminated soils has been frequently observed (Frossard and others 2018; Mahbub and others 2017c; Müller and others 2001). However, how Hg co-selects for ARGs within a non-agricultural soil community is not well understood. Therefore, we undertook this study to generate a baseline of how environmentally relevant Hg concentrations co-select for ARGs in soil not impacted by the application of animal manure or biosolids. We prepared microcosms of two different non-agricultural Australian soils spiked with different concentrations of inorganic Hg and aged them for 5 years. Following the aging period, we quantified the class 1 integron-integrase gene *intI1* (a gene capture system closely associated with ARGs and Hg resistance genes), *tetA* and *tetB* (tetracycline resistance genes), *sul1* (sulphonamide resistance gene), *dfrA1* (trimethoprim resistance gene), *vanB* (vancomycin resistance gene) and *qnrS* (quinolone resistance gene). Further, the bacterial community was characterised to identify shifts in the Hg contaminated microcosms and to establish links between soil parameters, Hg concentrations, ARG proliferation and the soil microbiota.

2. Methods

2.1.Soil sampling and characterization

Two soil samples were previously collected (Mahbub and others 2017b) at 0-10 cm depth in June 2014 from two different park-lands in Adelaide, SA, Australia. GPS co-ordinates for the neutral pH soil (called soil-N in this study) and the alkaline pH soil (called soil-A in this

study) were 34°48'30.8"S/138°37'20.9"E and 34°48'53.9"S/138°36'58.6"E respectively. Any vegetation and non-soil materials larger than 5 mm were removed by hand. The soils were then air dried for 5 d by spreading on a PVC tarp. Soil aggregates were broken by hand and a wooden hammer and, sieved at 2 mm before storage in closed PVC containers at 18 °C. Sieved soils were thoroughly homogenized before characterization. An oven drying method was employed to measure moisture content of air-dried soils. Soil texture was analysed by a micro pipetted method (Miller and Miller 1987). The maximum water holding capacity (%WHC) of the soils were determined by a published method (Gardner 1983). Soil pH was determined electrometrically on a 1:5 dry soil-water suspension after 2 h stirring using a glass membrane electrode at 25 °C. The electrical conductivity (EC) was determined with an EC probe in the aqueous extract of a 1:5 soil-water suspension and recorded in deciSiemens/m at 25 °C. Total organic carbon (TOC) and total nitrogen contents were determined using a Tru Mac (LECO, Japan) CNS elemental analyser.

2.2.Soil spiking

Stock solution of 5000 mg/L inorganic mercury (as $HgCl_2$) was used to spike 3 kg of each sieved and dried soil to the desired Hg concentrations maintaining 70% of total water holding capacity of soils. The Hg concentrations used for spiking were 5, 10, 50, 100, 150 and 200 mg/kg soil. A control soil containing deionized water only was prepared (0 mg/kg Hg). The spiked soils were mixed well in a soil mixing machine, kept and stored in covered PVC containers and aged for 5 y at 18 °C maintaining the moisture content to ~35%. The long-time ageing period was sufficient for the spiked Hg to obtain an equilibrium state in the soils thus mimicking field conditions.

2.3.Analysis of total and bioavailable fractions of mercury

After 5 years of ageing, total and water-soluble fractions of Hg in the spiked soil samples were determined. For total Hg content, 0.5 g soil was digested with aqua-regia in a CEM (Mars 6) digestion system following the US-EPA 3051a method. After digestion, the samples were diluted with 1% HCl up to 50 ml. For analysing water-soluble fractions of Hg from spiked soils, 5 g soil was mixed with 25 ml de-ionized water and shaken overnight in an end-over-end shaker. The soil extract was collected by centrifugation at 2000 *x g* for 20 min and then filtration with 0.45 µm cellulose nitrate filter. The water extract and aqua-regia digested soil samples were then analysed for Hg using inductively coupled plasma optical emission

158 spectrometry (ICP-OES, Perkin Elmer Avio 200, USA). The detection limit of Hg for this
159 instrument was 0.02 mg/L.

160 **2.4.DNA extraction and qPCR analyses**

161 Triplicate Soil DNA from homogenously mixed soils from each microcosm was extracted
162 using a Power Soil DNA Isolation kit (MoBio) following the manufacturer's protocol. DNA
163 concentrations were measured by a Qubit Flourometric Quantification Platform (Invitrogen).
164 Quantitative PCR (qPCR) was used to quantify the abundance of the marker for
165 anthropogenic pollution Class 1 integron-integrase gene (*intI1*) (Gillings and others 2008)
166 and the antibiotic resistance genes: *tetA* and *tetB* (conferring resistance to tetracyclines), *sul1*
167 (conferring resistance to sulphonamides), *qnrS* (conferring resistance to quinolones), *vanB*
168 (conferring resistance to vancomycin) and *dfrA1* (conferring resistance to trimethoprim) and
169 the 16S rRNA gene for total bacterial abundance (Berglund and others 2014).

170 Standards were created by amplifying sections of the respective genes by conventional PCR
171 from environmental samples, gel purifying them using the Isolate II PCR and Gel Kit, Bioline
172 and cloning them using the pGEM-T Easy Vector System (Promega). Ligations were
173 transformed into electro-competent *Escherichia coli* TOP10 cells (Invitrogen) using a
174 GenePulser Xcell (Bio-Rad) according to the manufacturer's protocols. Single colonies from
175 each ligation were chosen and the existence of the insert was verified by PCR. Plasmids
176 carrying these PCR products were then extracted (GenElute Plasmid Miniprep Kit, Sigma)
177 and measured using the Qubit Flourometric Quantification Platform (Invitrogen) and stored
178 at −20 °C.

179 Quantification was performed by qPCR using a BIORAD CFX384 Touch™ Real-Time PCR
180 Detection System™. Standard curves were prepared by serial dilution of the standards in
181 molecular grade water. All qPCR tests were run with three technical replicates, consisting of
182 5 µl reaction volumes containing 2.5 µl iTaq UniverSYBR Green SMX 2500®, 1.1 µl
183 molecular grade water, 0.2 µM for each forward and reverse primers (Supplementary Table
184 1) and 1 µl of diluted template DNA (1:4 for ARGs and 1:1000 for 16s rRNA gene) using an
185 epMotion® 5075l Automated Liquid Handling System. To quantify copy numbers of each
186 gene, the following qPCR cycling parameters were used: 95 °C for 180 s, followed by 39
187 cycles of a 2-step reaction involving denaturation at 95 °C for 15 s and annealing/extension
188 step at 58 °C for 30 s (for *tetA*), 60 °C for 30 s (for *intI1* and *tetB*), 60 °C for 60 s (for *vanB*),
189 61 °C for 30 s (for *qnrS*), 62°C for 30 sec (for *dfr1A*), 65 °C for 30 sec (for *sul1*). A three-

step reaction of 95 °C for 15 s, 55 °C for 30 s and 72 °C for 15 s was employed for the 16S rRNA gene. The amplifications were followed by a holding stage at 72 °C for 120 s and a melting curve to confirm that there was no non-specific binding. Negative controls were included in each qPCR plate for detecting any contamination. Copy numbers of each amplicon were calculated against their standard curves using the BIORAD CFX Manager Software. All gene copy numbers were normalized to per kg of soil. Normalised abundance of the ARGs and *intI1* were calculated from the ratio of the absolute copy numbers of the ARGs and 16S rRNA gene. All reagents and qPCR plate preparation were performed in an automated liquid handling platform (epMotion 5075I).

2.5.16S rRNA amplicon-based sequencing of the experimental soils' DNA

Triplicate DNA samples from control and spiked soils were subjected to 16S rRNA amplicon sequencing to characterise changes in bacterial composition and to establish potential links with ARGs in the clean and contaminated soils. The V1-V3 variable region of the bacterial 16S rRNA gene was amplified by PCR, using the primers 27F (AGAGTTTGATCMTGGCTCAG, (Lane 1991)) and 519R (GWATTACCGCGGCKGCTG, (Turner and others 1999)) and sequencing was performed on the Illumina MiSeq platform at the Ramaciotti Centre for Genomics at University of New South Wales, Australia. Demultiplexed raw FASTQ reads were deposited in MG-RAST database with accession numbers mentioned in Supplementary Table 2.

2.6.Bioinformatics

The downstream processing of demultiplexed FASTQ paired end sequences obtained from the 16S rRNA amplicon sequencing was carried out in QIIME2 (Bolyen and others 2018). Briefly, sequences were first imported and then denoised using DADA2 (Callahan and others 2016). Taxonomy was then assigned using the sklearn QIIME feature-classifier (Bokulich and others 2018) against the Silvav132 database (https://www.arb-silva.de/) and sequences were clustered at the single nucleotide level (zero-radius OTUs; zOTUs) (Edger 2018). Sequences assigned as mitochondria and chloroplasts were filtered from the dataset.

2.7.Statistical analyses

Linear regression analysis and a one-way ANOVA with Tukey's Honest Significant Difference (HSD) Post Hoc test were conducted for spiked and measured Hg concentrations in soil microcosms. The threshold percent coefficient of variation (%CV) of technical

replicates was maintained below 2%. Any significant difference between the means of relative abundance of the measured ARGs in the soils were tested by one-way ANOVA and Fisher's Least Significant Difference (LSD) Post-Hoc analysis. All statistical analyses for soil and ARG analyses were performed using SPSS.

For the 16S rRNA amplicon sequencing data, the differences in alpha diversity indices, including observed OTUs, Shannon index, evenness, and Faith's Phylogenetic Diversity (faith-pd) among different samples were analysed using a Kruskal–Wallis H test in the QIIME 2 statistical environment. The permutational multivariate analysis of variance (PERMANOVA) analysis in the QIIME 2 was employed to determine differences in beta diversity indices namely Jaccard, Bray-Curtis, Unweighted, and Weighted UniFrac methods. Relative abundance of phyla was analysed in STAMP. SIMPER analysis was performed in PAST3 to identify the taxa that most responsible for driving dissimilarity between 16S rRNA community profile. Canonical correspondence analysis (CCA) was performed in PAST3 to investigate correlation between the soil parameters and ARG abundances with bacterial abundance.

3. Results and Discussion

3.1.Soil properties

The two soils used in the present study principally varied in pH with soil-N denoting a neutral pH soil and soil-A denoting an alkaline pH soil (Table 1). EC values also differed between the two soils with substantially higher EC in soil-N. WHC, N, TOC and clay content were similar in the two experimental soils. Thus, the soils used in the study contrasted only on pH and EC values, parameters that are known to be important in mercury bioavailability and toxicity in terrestrial environments.

Table 1: Characteristics of soils used in this study

Soil	pH	EC (µs/cm)	% WHC	% TOC	% N	% Sand	% Silt	% Clay
Soil-N	7.2 ± 0.05	323 ± 10	41.9 ± 2	2.1 ± 0.01	0.23 ± 0.001	51.2 ± 2	35.7 ± 2	13 ± 2
Soil-A	8.5 ± 0.04	232 ± 10	38.6 ± 2	2.2 ± 0.01	0.22 ± 0.001	42.0 ± 2	44.3 ± 2	13.6 ± 2

Note: EC= electrical conductivity, WHC=water holding capacity, TOC=total organic carbon, N=nitrogen. The values are mean±SD (n=3).

3.2. Mercury chemistry in the experimental soils and its attenuation after 5 years of aging

Total mercury (THg) content in the spiked microcosms of soil-N varied from 0.29 mg/kg (equivalent to background level) to 35 mg/kg (Figure 1A). In soil-A, these contents varied from 0.46 mg/kg (equivalent to background level) to 56 mg/kg (Figure 1B). A positive linear correlation (R^2=0.93) was observed between the spiked amounts and recovered amounts of Hg in both soils. The recoveries of THg in both soils were significantly different from the control soils with no added Hg ($p<0.05$) in all microcosms. While comparing the means of Hg recovery between the microcosms of the two soils, it was observed that Hg recovery was similar in microcosms that contained initial amounts of 5 and 10 mg/kg Hg ($p>0.05$). This indicates that 5 years of ageing might have caused volatilization of bioavailable Hg fractions. Following volatilization the total Hg content in these two microcosms reached to the same level. Overall a decrease in THg content was observed in all microcosms after 5 years of ageing, compared to total Hg contents in these soils measured after 3 months of spiking in a previous study (Mahbub and others 2017b); and this loss in THg content over 5 years was calculated at 58-81%, and 34-72% for soil-N and soil-A respectively. This was anticipated, because natural attenuation of metals by biotic and abiotic volatilization from contaminated lands is a common phenomenon (Mulligan and Yong 2004). Since these soils were kept at room temperature with ~35% moisture content, it is expected that Hg resistant bacteria increased over time and enzymatically reduced Hg^{2+} to Hg^0 leading to its volatilization. The variation in the percentage of loss may be linked to soil properties, as the loss was higher in the neutral pH soil. The neutral pH soil might have favoured the bacterial community for higher metabolic activity than that in the alkaline pH soil.

As total metal content does not reflect the biologically relevant concentration of a metal in soil, we attempted to measure water-soluble fractions in the microcosms, which is more relevant to the bioavailability of Hg in a contaminated soil. However, we could not measure any detectable amount of water-soluble Hg in the spiked microcosms. This is because only a negligible amount of Hg in the soluble fractions of the spiked soils is left after natural attenuation. This observation is consistent with previous studies that have reported very little or no water soluble Hg fractions in contaminated soils because of its strong association with clay minerals and organic substances (de Vries and others 2007; Mahbub and others 2016a).

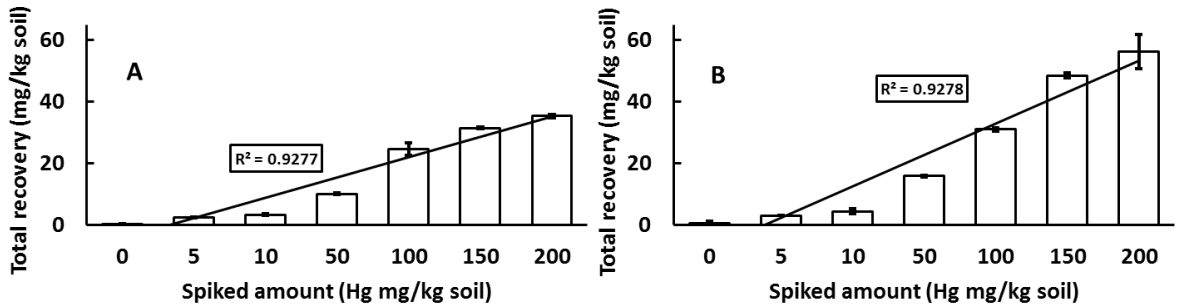

277

278 **Figure 1:** Recovery of total mercury from spiked soils after 5 years of ageing; A) soil-N, B)
279 soil-A. Error bars represent standard deviation of the mean (n=3), some error bars are too
280 small to be visible. Regression lines demonstrate a linear correlation between spiked amounts
281 and recovered amounts after the ageing period.

282

283 **3.3.Influence of Hg on the abundance of the tested genes in the soil microcosms**

284 In this study, two non-agricultural soils of varying physicochemical properties collected from
285 two recreational parks and spiked with gradually increased Hg concentrations were
286 investigated to determine whether a correlation between Hg and ARGs was present. The
287 qPCR analyses of 16S rRNA, ARGs and *intI1* genes produced varying results in the
288 experimental microcosms of the two different soils.

289 ***3.3.1. Hg effect on the abundance of 16S rRNA genes***

290 In both soils, 16S rRNA gene copy numbers, used here as a proxy for total bacterial
291 abundance, were similar in the control microcosms ($p>0.05$) (Figure 2). In the Hg spiked and
292 control microcosms of soil-N, 16S rRNA gene copy numbers did not vary significantly
293 ($p>0.05$). However, in soil-A, there was a significant increase (approximately 10-fold,
294 $p<0.05$) in 16S rRNA gene copy in the Hg spiked microcosms compared to the control
295 microcosm containing background levels of Hg. There was no or small differences in copy
296 numbers within the Hg spiked microcosms in soil-A. 16S rRNA gene counts indicated that in
297 the neutral pH soil, total bacterial abundance was not affected by Hg contamination.
298 However, an effect was observed in soil-A where Hg spiking caused a significant increase in
299 the 16S rRNA gene count. This could be explained by the ageing affect and varying soil
300 chemistry. In the contaminated neutral pH soil, the bacterial composition might have reached
301 an equilibrium state equivalent to the control soil after 5 years of aging since Hg effects
302 might have been reduced due to microbial detoxification. However, in alkaline soil-A, Hg

might have facilitated the growth of certain bacterial groups, which outnumbered the initial microbiota in that soil. Such increases in total bacterial quantity in Hg contaminated soil is consistent with increased microbial activity in long term Hg contaminated sites (Campos and others 2018), although decreased microbial activity in Hg contaminated soil is also frequently reported (Casucci and others 2003; Yang and others 2007).

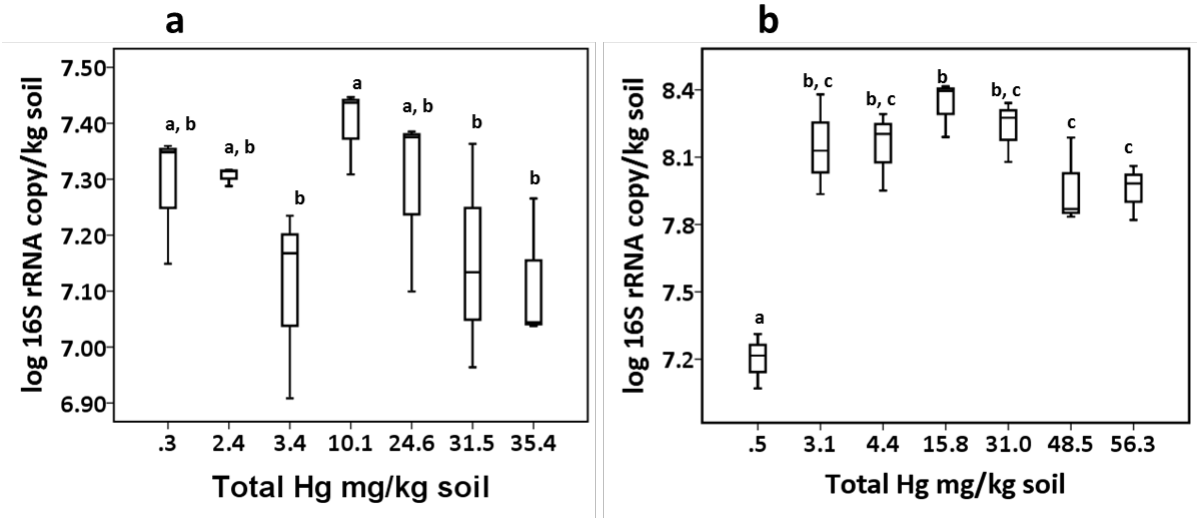

Figure 2: Absolute count of 16S rRNA genes in the experimental microcosms – a) soil-N and b) soil-A. The absolute copy numbers were log transformed and presented as boxplots. Horizontal bars are median values (n=3) and the whiskers represent upper and lower limits. Means (n=3) that do not share a letter are significantly different ($p<0.05$). There were no outliers in the dataset.

3.3.2. ARGs are ubiquitous in the tested soils

All ARGs, except *vanB* and *qnrS* were detected in both the experimental control and Hg contaminated soils, while their abundance varied differently in the microcosms of the two soils. *dfrA1* gene was detected in soil-N only. Their absolute counts per kg soil and relative abundance (ratio with 16S rRNA genes) are presented in Figures 3 and 4 respectively. The relative abundance of *int1I, tetA, tetB*, *sul1* and *dfrA1* in the control microcosms of soil-N were approximately 10^{-5}, 10^{-4}, 10^{-4}, 10^{-4} and 10^{-5} respectively. On the other hand, in control microcosm of soil-A, relative abundance of *intI1, tetA, tetB* and *sul1* were approximately 10^{1}, 10^{-4}, 10^{-2} and 10^{-4} respectively. The presence of ARGs and *intI1* genes in the control soils in the present study supports the previous reports of natural occurrence of ARGs in soils impacted by anthropogenic activities (D'Costa and others 2011). Additionally, ARGs harboured in the diverse soil microbial community can be increased by selection/co-selection by contamination and therefore, serving as a potential reservoir for LGT mediated

dissemination into animals and humans. The absence of *vanB* gene in soil was expected since this gene is rarely detected in the environment (Carney and others 2019; Li and others 2015). Vancomycin is a last resort antibiotic used for treating Gram positive pathogens (Arias and Murray 2012) and the absence of *vanB* gene in our experimental soils reflects the restriction of vancomycin use in Australia. The *qnrS* gene confers resistance to quinolone which is also a controlled antibiotic in human and veterinary practices in Australia (Cheng and others 2012). Nevertheless, it is more likely found in wastewater treatment plants (Colomer-Lluch and others 2014) hence, its absence in non-agricultural soil environments is not a surprise.

3.3.3. Hg co-selects for ARGs in alkaline soil

The abundance of *intI1* was similar ($p>0.05$) in the control microcosms of the two soils (Figure 3a). However, the absolute copy numbers of *intI1* decreased ($p<0.05$) in the microcosms containing 31.5 and 35.4 mg/kg Hg in soil-N, whereas in soil-A, Hg contamination was found to cause a significant increase in *intI1* copy numbers ($p<0.05$). In soil-A, 3.1 mg/kg Hg caused a 1000 fold increase in *intI1* ($p<0.05$) and remained relatively unchanged as Hg concentrations increased ($p>0.05$). *intI1* is used as a proxy molecular marker for ARG abundance in terrestrial and aquatic sites contaminated with metals, sewage and disinfectants (Gillings and others 2015; Koczura and others 2016). A 1000-fold increase in *intI1* in the Hg contaminated microcosms of soil-A indicates selection pressure by Hg co-selects for ARGs.

A similar pattern to that observed with *intI* was apparent in the tetracycline resistance *tetA* gene (Figure 3b), with the abundance of this gene decreasing with increasing Hg concentrations in soil-N but slightly increased with increasing Hg contents (at 3.1 to 15.8 mg/kg Hg) in soil-A compared to the respective control soils ($p<0.05$). The relative abundance of *tetA* gene was similar in both control soils ($\sim10^{-4}$, $p>0.05$). Another tetracycline resistance gene, *tetB,* decreased in the Hg contaminated soil-N but increased at 15.8 mg/kg Hg in soil-A ($p<0.05$) (Figure 3c). Various tetracycline resistance genes including *tetA* and *tetB* are widely detected in manure impacted agricultural soils and waste water treatment plants (Ji and others 2012). In a previous study, the *tetB* gene was found to be co-selected in agricultural soils contaminated with arsenic (As) but had no correlation with Hg in the same soil (Ji and others 2012) while another study found positive correlation of Hg contamination and *tet* genes (Gorovtsov and others 2018).

The *sul1* and *dfrA1* genes confer resistance to sulphonamides and trimethoprim, two synthetic antibiotics commonly used in combination to treat many human infections (Richards and others 1996). In our study, Hg did not affect *sul1* abundance in soil-N ($p>0.05$), but in soil-A

there was a significant reduction ($p<0.05$) (Figure 3d). Contrasting results were observed in a few previous studies that reported positive correlations of Hg (and Zn and Cu) with sulphonamide resistance genes in manured agricultural soils (Gorovtsov and others 2018; Ji and others 2012). *dfrA1* was detected only in soil-N showing no Hg associated co-selection in the experimental microcosms (Figure 3e).

In this study, *intI1*, *tetA* and *tetB* genes were co-selected at certain concentrations of Hg contaminated alkaline soil-A. A decrease in the absolute copy numbers of *sul1* in soil-A were observed in high Hg concentrations indicating Hg toxicity to sulphonamide resistant bacteria in these soils. Whereas, in the neutral soil-N, there was no evidence of co-selection despite having similar Hg concentrations as in soil-A. Soil pH is known to determine the bioavailability and toxicity of soil bound Hg and its subsequent impact on soil microbiota (de Vries and others 2007). The contrasting results in the two experimental soils indicate a possible combined role for soil pH-Hg chemistry in facilitating the outgrowth of microbial hosts in soil-A that harboured these genes or a possible variation in the starting composition of microflora in these two soils. To understand this phenomenon, we performed bacterial community analyses and investigated links between the soil microbiota, soil parameters and the co-selection of ARGs in the following sections.

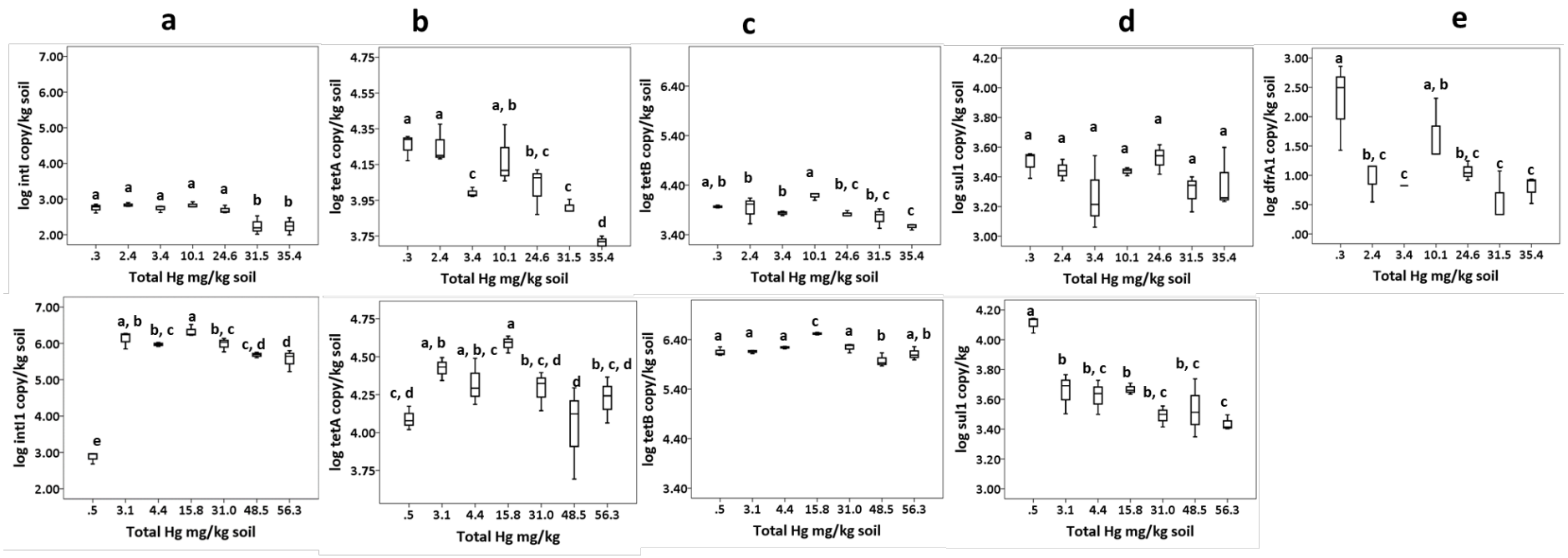

Figure 3: Absolute copy numbers of ARGs and *intI1* in two experimental soils contaminated with increasing concentrations of Hg. Upper and lower panels represent soil-N and soil-A respectively. The gene copy numbers in per kg soil are log transformed and presented as boxplots. The horizontal bars in the boxplots are the median values and the whiskers represent upper and lower limits. Tested Hg concentrations demonstrated varying correlations with a) *intI1*, b) *tetA*, c) *tetB*, d) *sul*1 and e) *dfrA*1. Means (n=3) that do not share a letter are significantly different ($p<0.05$). There were no outliers in the dataset.

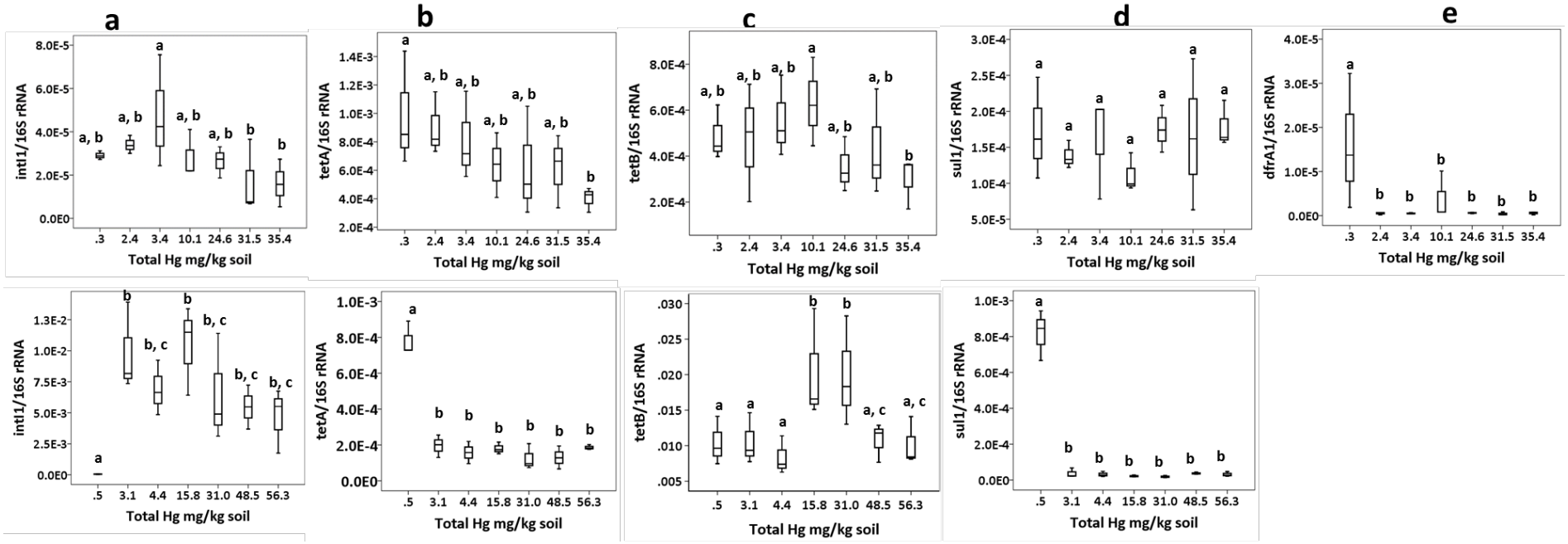

Figure 4: Relative abundance of ARGs and *intI1* in two experimental soils contaminated with increasing concentrations of Hg. Upper and lower panels represent soil-N and soil-A respectively. The ARG copy numbers were divided by 16S rRNA copy numbers and presented as boxplots. The horizontal bars in the boxplot are the median values and the whiskers represent upper and lower limits. Tested Hg concentrations demonstrated varying correlations with a) *intI*1, b) *tetA*, c) *tetB*, d) *sul*1 and e) *dfrA*1. Means (n=3) that do not share a letter are significantly different ($p<0.05$). There were no outliers in the dataset.

3.4. Bacterial community diversity in the control soils and soils with moderate concentrations of mercury

We chose the control microcosms and microcosms with 24.6 mg/kg Hg of soil-N (initially spiked amount was 100 mg/kg) and 31 mg/kg Hg of soil-A (initially spiked amount was 100 mg/kg) for analyses of bacterial community by amplicon-based sequencing of 16S rRNA genes. We selected these microcosms for the following reasons: a) these concentrations represent Hg content in many contaminated terrestrial sites (Kim and others 2016; Müller and others 2001; Zhu and others 2018); b) similar concentrations impact plants, invertebrates and microbes in previous studies (Mahbub and others 2016a; Mahbub and others 2017b; Mahbub and others 2016b) and c) the results obtained by qPCR analyses indicate that these two concentrations caused significant changes in the abundance of *intI1*, *tetA* and *tetB* in the experimental soils. Triplicate soil samples from the selected microcosms were subjected to DNA extraction and 16S rRNA gene sequencing and subsequent downstream processing of data for statistical and bioinformatics analyses.

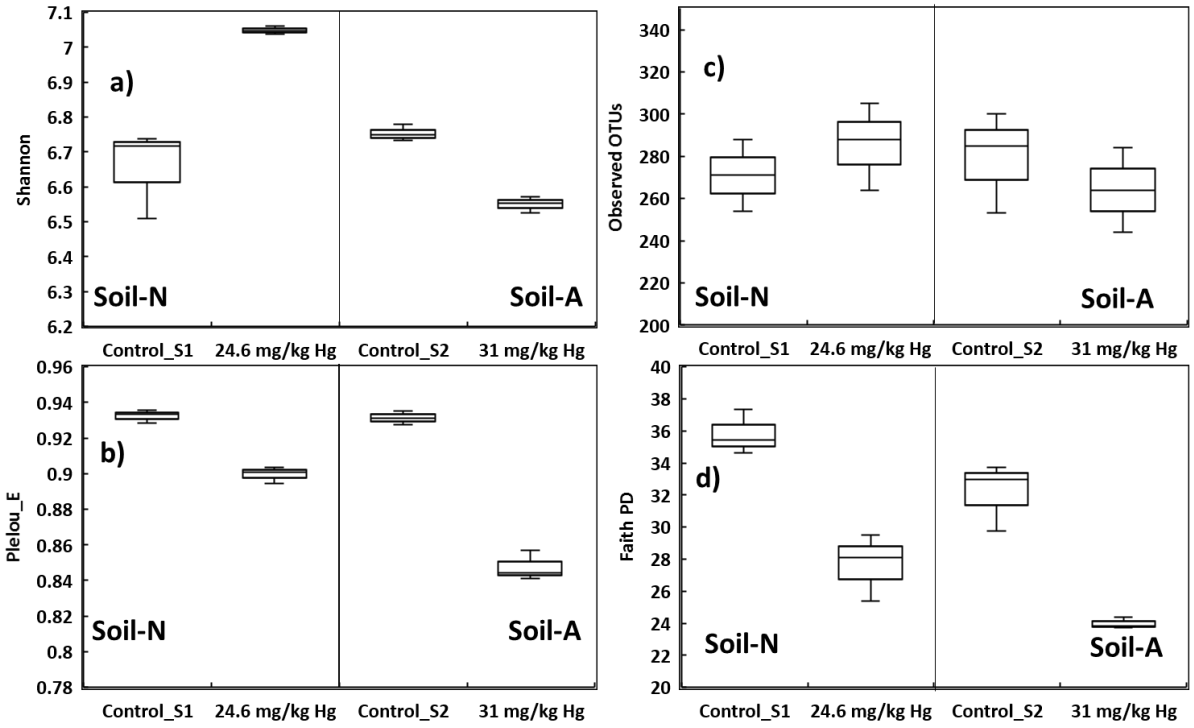

Figure 5: Bacterial alpha diversity in the experimental microcosms of two soils – a) Shannon index, b) Plelou's evenness, c) Observed OTUs and d) Faith PD. Data from triplicate samples are presented in box and whisker plots.

A total of 315,461 raw sequencing reads were initially obtained. After denoising and cleaning the sequencing data, 101,267 bacterial raw reads were kept. Reads were then filtered to

remove mitochondrial and eukaryotic reads and low frequency reads (0.01%). After rarefaction to sampling depth of 5658, 67,896 clean reads were obtained and subjected to further analyses. Queries of these reads to the Silva database generated a total of 1443 zOTUs across samples from 12 replicates of 4 microcosms. Minimum, maximum, mean and median frequencies of the zOTUs across the samples were 3, 3227, 47.05 and 19 respectively.

The alpha diversity of the microbiota was impacted significantly by Hg contamination in both soils (Figure 5). Compared with the controls, the Kruskal–Wallis H test revealed that the Shannon index increased in Hg spiked soil-N ($p=0.04$, $H=3.85$, $q=0.06$) but decreased in the Hg spiked soil-A ($p=0.04$, $H=3.85$, $q=0.06$). The Plelou's evenness significantly decreased in the Hg contaminated microcosms of both soils ($p=0.04$, $H=3.85$, $q=0.06$). The Faith PD significantly decreased in the Hg contaminated microcosms of both soils ($p=0.04$, $H=3.85$, $q=0.05$). However, there were no significant changes in observed OTUs between the controls and Hg treated microcosm in soil-N ($p=0.38$, $H=0.78$, $q=0.62$) and soil-A ($p=0.28$, $H=1.2$, $q=0.61$).

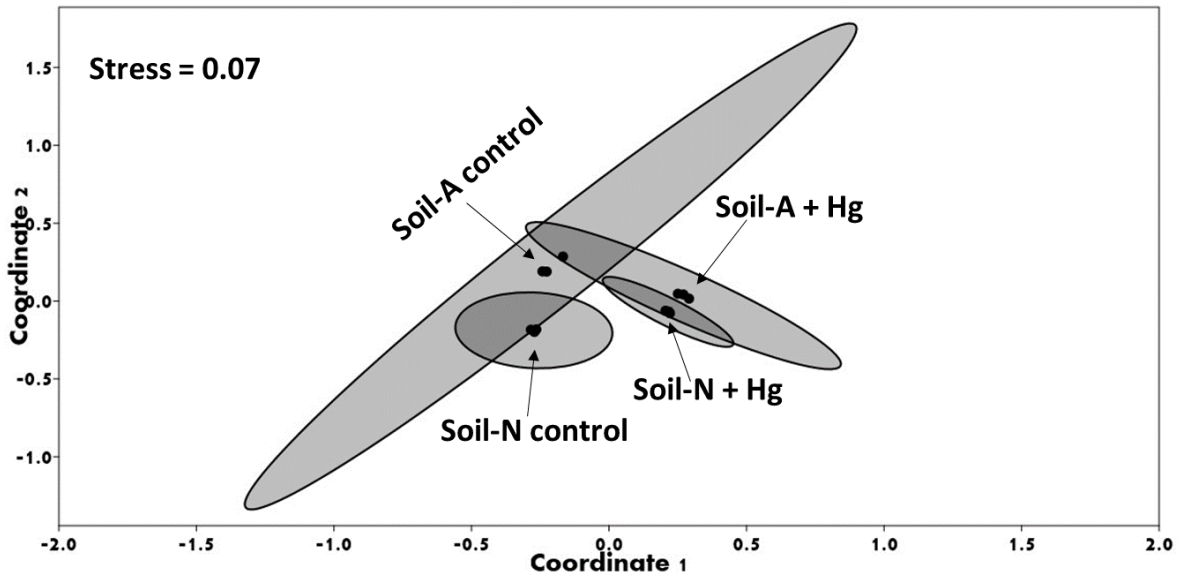

Figure 6: Two dimensional nMDS plot showing a significant separation of the microbiota in the experimental microcosms. The ellipses are at 95% confidence limit. The microbiota was separated based on Hg treatment and soil location.

Beta diversity analyses namely Jaccard Distance, Bray-Curtis Distance, Unweighted Uni-Frac Distance and Weighted Uni-Frac Distance all demonstrated a dissimilarity between the microbiotas from controls and Hg-treatments in both experimental soils (Supplementary

Figure 1). A nonmetric multidimensional scaling (nMDS) with PERMANOVA analysis demonstrated significant separation of the control soils with their respective Hg treated microcosm and also a separation between the control groups (Figure 6). The separation of the microbiotas of the control soils indicates that the natural microbiota in the two soils were also different. Hg associated diversity shift in soil microflora has previously been reported (Frossard and others 2018; Mahbub and others 2017c). Such changes in diversity indicates the outgrowth of microbes in the contaminated soils that were already resistant or evolved Hg resistance (e.g. through LGT) to survive Hg stress and hence may have played a role in the natural attenuation of Hg observed in the present study. Additionally, these Hg resistant microbial groups may carry co-selected ARGs in their metal resistant plasmids or transposons.

3.5.Bacterial taxa that contributed to the community diversity in the microcosms

In the control and treated microcosms of soil-N and soil-A, 19 and 17 phyla were detected respectively (Supplementary Figure 2). A SIMPER analysis (Supplementary File 1) of the abundant phyla with Bray-Curtis distance measure in PAST3 indicated an overall average dissimilarity of 23.47 % and 25.08 % between the microbiotas of controls and treatments of soil-N and soil-A respectively. An 18.68 % overall average dissimilarity was also observed between the uncontaminated control soils. The shifted microbiotas in the two Hg contaminated soils were only 11 % different (overall average dissimilarity), indicating a high similarity between the Hg resistant bacteria enriched or evolved in the two different soils. At zOTU level the dissimilarity was 83.39 % and 84.51 % in soil-N and soil-A respectively. The SIMPER analyses result at zOTU level, genus level and phylum level are presented in Supplementary File 1.

In the soil-N microcosms, *Proteobacteria* were responsible for the highest dissimilarity of 28.94 % between the contaminated and uncontaminated soils. The contribution of other phyla towards dissimilarity in microbiota in soil-N were *Bacteroidetes* (18.96 %), *Actinobacteria* (14.31 %), *Firmicutes* (7.4 %), *Chloroflexi* (7 %), *Patescibacteria* (6.9 %), *Dentotheonellaeota* (3.89 %), *Gemmatimonadetes* (3.53%), *Spirochaetes* (1.91 %), *Acidobacteria* (1.54 %), *Planctomycetes* (1.38 %), *Hydrogenedentes* (1.1 %), *Armatimonadetes* (1.1 %), *Dependentiae* (0.58 %), *Elusimicrobia* (0.44 %), *Nitrospirae* (0.38 %), *Verrucomicrobia* (0.26 %), *Omnitrophicaeota* (0.25 %) and *Bacteria* (0.15 %).

In soil-A, *Bacteroidetes* (23.91 %) was the main driver toward community dissimilarity in the controls and treatments, followed by *Proteobacteria* (22.85 %), *Chloroflexi* (11.31 %),

Actinobacteria (10.39 %), *Patescibacteria* (10.21 %), *Gemmatimonadetes* (7.6 %), *Acidobacteria* (3.4 %), *Planctomycetes* (2.3 %) *Dentotheonellaeota* (2.2 %), *Spirochaetes* (1.8 %), *Firmicutes* (1.5 %), *Elusimicrobia* (0.92 %), *Hydrogenedentes* (0.87 %), *Nitrospirae* (0.34 %) *Dependentiae* (0.21 %) and *Armatimonadetes* (0.08 %).

3.6. The soil nitrogen cycle may be affected by mercury contamination

The *Nitrospirae* phylum was negatively affected by Hg in both soils (Supplementary Figure 3). *Nitrospirae* is composed of bacteria responsible for maintaining the nitrogen cycle (performing nitrite oxidation in the second step of nitrification) in soils having great impact on soil fertility (Bates and others 2011). *Nitrospirae* were inhibited when the experimental soils were initially spiked (Mahbub and others 2017c) and did not revive after 5 years of aging, indicating high sensitivity to Hg contamination for these agriculturally important soil bacteria. Hence, *Nitrospirae* could be used as a biomarker to assess Hg toxicity in soil or in an attempt to restore the function of contaminated soils, added back through seeding with healthy soil.

3.7.Shifts in soil bacterial communities show links to Hg contamination and the co-selection of ARGs

A Canonical Correspondence Analysis (CCA) identified a strong association ($p = 0.002$) among the multiple variables including the abundant phyla, quantified ARG copy numbers and environmental parameters (Figure 7). Hg was observed to exert the highest effect on the soil microbial community and ARGs as evident by the largest vector in the CCA triplot. Among the bacterial phyla, *Protoeobacteria*, *Bacteroidetes* and *Planctomycetes* were strongly correlated with soil Hg content, soil pH and TOC (Figure 7). Noteworthy is the strong positive association of Hg content, soil pH and TOC and those bacterial phyla with *intI1*, *tetA* and *tetB* genes which were co-selected by Hg and a negative correlation with *sul1* gene that was not co-selected (Figure 4). Although, *intI1* and *sulI* are often co-located in ARG loci from clinical pathogens, it is the case that *intI1* is commonly found independent of *sul1* in both clinical and in the wider environment (Rosser and Young 1999).

The strong association of *Proteobacteria*, *Bacteroidetes* and *Planctomycetes* with soil Hg indicates the proliferation of these groups in Hg contaminated soils which might have evolved Hg resistance traits. We performed a STAMP post-hoc analysis of the relative abundance of these three groups within the microcosms showing a significant increase of *Proteobacteria* ($p<0.01$), *Bacteroidetes* ($p<0.01$) and *Planctomycetes* ($p<0.05$) in the Hg treated microcosms (Supplementary Figure 4). The dominance of resistant groups of community to maintain ecological stability in pollution affected environment is a common

phenomenon (Girvan and others 2005). When the bacterial community was analysed in a previous study in the same soils after immediate (3 months) exposure to Hg, both *Proteobacteria* and *Planctomycetes* were positively correlated with Hg (Mahbub and others 2017c) and this pattern remained the same after 5 years. In other studies, these groups of bacteria were often reported to contain Hg resistant microbes in soil environments (Frossard and others 2017; Száková and others 2016). Moreover, the strong association of the co-selected ARGs with these bacterial groups in the present study indicates potential co-selection of antibiotic resistance genetic traits among these Hg resistant phyla. Such co-selection might have occurred due to increased LGT rate or mutation under Hg stress or outgrowth of bacteria that carry both Hg resistance genes and ARGs. However, it is still not clear whether LGT occurs in a greater rate in metal contaminated soil as a recent study showed that resistance MGEs such as Hg resistance transposons bearing plasmids are less mobile under Hg selection pressure in soil (Hall and others 2017). This reduction in plasmids' mobility is attributed to the killing of recipient soil bacterial communities because of their sensitivity to Hg toxicity.

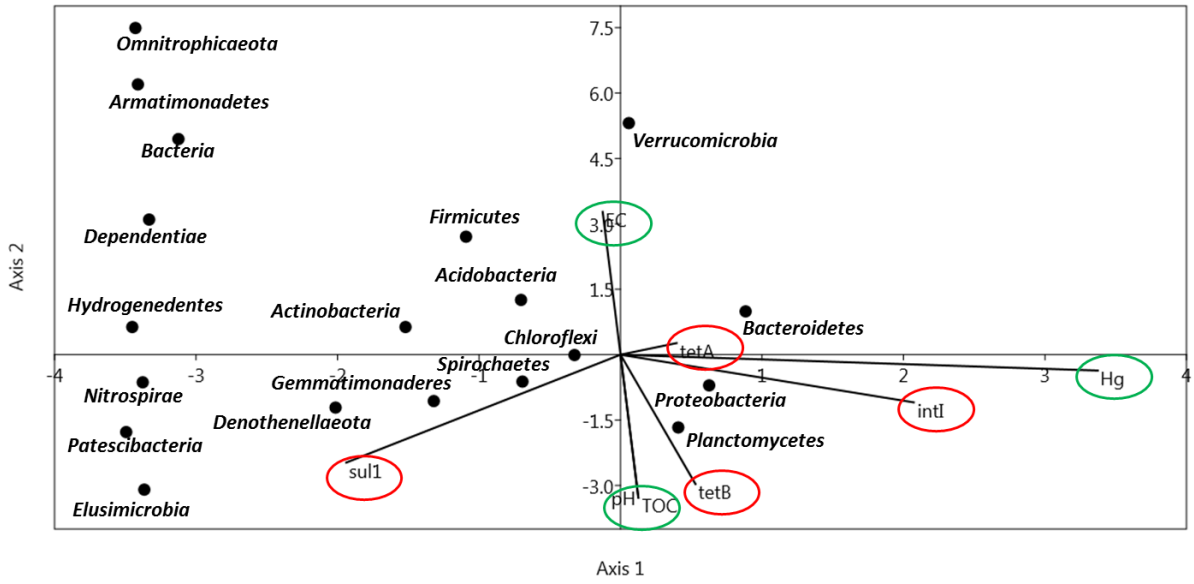

Figure 7: CCA triplot of the abundant phyla (black dots) with environmental parameters and ARGs in the soils. The vectors moving outward represent environmental parameters (green circles) and quantified genes (red circles). Axis 1 (eigenvalue 0.08) and Axis 2 (eigenvalue 0.03) represent 66.03% and 22.66% of data. A significant association was observed between the parameters tested (p=0.002, permutation N=999).

4. Conclusions

This study demonstrates that certain concentrations of soil bound-Hg can co-select for several ARGs in terrestrial environments that are not impacted by agricultural activities. ARG co-selection is influenced by soil properties (e.g. pH) likely due to the interaction of Hg with soil particles. This highlights the potential variable nature of the co-selection of ARGs in Hg contaminated sites, which will influence the degree to which metal contaminated soils act as a reservoir of antibiotic resistant bacteria. This research highlights the need to consider multiple aspects of soil chemistry, as well as Hg contamination when investigating the prevalence of ARGs in Hg contaminated terrestrial sites.

5. Acknowledgement

The research was supported by an Australian Research Council Linkage grant (ARC LP140100459).

6. Declarations of Interest

None.

References

Arias, C.A.; Murray, B.E. The rise of the Enterococcus: beyond vancomycin resistance. Nature Reviews Microbiology. 10:266; 2012

Baker-Austin, C.; Wright, M.S.; Stepanauskas, R.; McArthur, J. Co-selection of antibiotic and metal resistance. Trends in microbiology. 14:176-182; 2006

Bates, S.T.; Berg-Lyons, D.; Caporaso, J.G.; Walters, W.A.; Knight, R.; Fierer, N. Examining the global distribution of dominant archaeal populations in soil. The ISME journal. 5:908; 2011

Berglund, B.; Khan, G.A.; Weisner, S.E.; Ehde, P.M.; Fick, J.; Lindgren, P.-E. Efficient removal of antibiotics in surface-flow constructed wetlands, with no observed impact on antibiotic resistance genes. Science of the total environment. 476:29-37; 2014

Bjørklund, G.; Dadar, M.; Mutter, J.; Aaseth, J. The toxicology of mercury: Current research and emerging trends. Environmental research. 159:545-554; 2017

Bokulich, N.A.; Kaehler, B.D.; Rideout, J.R.; Dillon, M.; Bolyen, E.; Knight, R.; Huttley, G.A.; Caporaso, J.G. Optimizing taxonomic classification of marker-gene amplicon sequences with QIIME 2's q2-feature-classifier plugin. Microbiota. 6:90; 2018

Bolyen, E.; Rideout, J.R.; Dillon, M.R.; Bokulich, N.A.; Abnet, C.; Al-Ghalith, G.A.; Alexander, H.; Alm, E.J.; Arumugam, M.; Asnicar, F. QIIME 2: Reproducible, interactive, scalable, and extensible microbiota data science. PeerJ Preprints; 2018

Callahan, B.J.; McMurdie, P.J.; Rosen, M.J.; Han, A.W.; Johnson, A.J.A.; Holmes, S.P. DADA2: high-resolution sample inference from Illumina amplicon data. Nature methods. 13:581; 2016

Campos, J.; Esbrí, J.; Madrid, M.; Naharro, R.; Peco, J.; García-Noguero, E.; Amorós, J.; Moreno, M.; Higueras, P. Does mercury presence in soils promote their microbial activity? The Almadenejos case (Almadén mercury mining district, Spain). Chemosphere. 201:799-806; 2018

Carney, R.L.; Labbate, M.; Siboni, N.; Tagg, K.A.; Mitrovic, S.M.; Seymour, J.R. Urban beaches are environmental hotspots for antibiotic resistance following rainfall. Water Research:115081; 2019

571 Casucci, C.; Okeke, B.C.; Frankenberger, W.T. Effects of mercury on microbial biomass and enzyme
572 activities in soil. Biological trace element research. 94:179-191; 2003
573 Cheng, A.C.; Turnidge, J.; Collignon, P.; Looke, D.; Barton, M.; Gottlieb, T. Control of
574 fluoroquinolone resistance through successful regulation, Australia. Emerging infectious
575 diseases. 18:1453; 2012
576 Colomer-Lluch, M.; Jofre, J.; Muniesa, M. Quinolone resistance genes (qnrA and qnrS) in
577 bacteriophage particles from wastewater samples and the effect of inducing agents on
578 packaged antibiotic resistance genes. Journal of Antimicrobial Chemotherapy. 69:1265-1274;
579 2014
580 D'Costa, V.M.; King, C.E.; Kalan, L.; Morar, M.; Sung, W.W.; Schwarz, C.; Froese, D.; Zazula, G.;
581 Calmels, F.; Debruyne, R. Antibiotic resistance is ancient. Nature. 477:457; 2011
582 Dash, H.R.; Das, S. Bioremediation of mercury and the importance of bacterial mer genes.
583 International Biodeterioration & Biodegradation. 75:207-213; 2012
584 de Vries, W.; Lofts, S.; Tipping, E.; Meili, M.; Groenenberg, J.E.; Schütze, G. Impact of soil
585 properties on critical concentrations of cadmium, lead, copper, zinc, and mercury in soil and
586 soil solution in view of ecotoxicological effects. Reviews of Environmental Contamination
587 and Toxicology: Springer; 2007
588 Edger, R.C. Updating the 97% Identity threshold for 16S ribosomal RNA OTUs. Bioinformatics.
589 34:2371-2375; 2018
590 Frossard, A.; Donhauser, J.; Mestrot, A.; Gygax, S.; Bååth, E.; Frey, B. Long-and short-term effects
591 of mercury pollution on the soil microbiota. Soil Biology and Biochemistry. 120:191-199;
592 2018
593 Frossard, A.; Hartmann, M.; Frey, B. Tolerance of the forest soil microbiota to increasing mercury
594 concentrations. Soil Biology and Biochemistry. 105:162-176; 2017
595 Gardner, W. Water content. Methods of soil analysis: Part 1. Physical and mineralogical properties,
596 including statistics of measurement and sampling, ed. CA Black Am Soc Agron Madison,
597 Wisconsin. 82:127; 1983
598 Gillings, M.; Boucher, Y.; Labbate, M.; Holmes, A.; Krishnan, S.; Holley, M.; Stokes, H.W. The
599 evolution of class 1 integrons and the rise of antibiotic resistance. Journal of bacteriology.
600 190:5095-5100; 2008
601 Gillings, M.R.; Gaze, W.H.; Pruden, A.; Smalla, K.; Tiedje, J.M.; Zhu, Y.-G. Using the class 1
602 integron-integrase gene as a proxy for anthropogenic pollution. The ISME journal. 9:1269;
603 2015
604 Girvan, M.; Campbell, C.; Killham, K.; Prosser, J.I.; Glover, L.A. Bacterial diversity promotes
605 community stability and functional resilience after perturbation. Environmental microbiology.
606 7:301-313; 2005
607 Gorovtsov, A.V.; Sazykin, I.S.; Sazykina, M.A. The influence of heavy metals, polyaromatic
608 hydrocarbons, and polychlorinated biphenyls pollution on the development of antibiotic
609 resistance in soils. Environmental Science and Pollution Research. 25:9283-9292; 2018
610 Hall, J.P.; Williams, D.; Paterson, S.; Harrison, E.; Brockhurst, M.A. Positive selection inhibits gene
611 mobilization and transfer in soil bacterial communities. Nature ecology & evolution. 1:1348;
612 2017
613 Ji, X.; Shen, Q.; Liu, F.; Ma, J.; Xu, G.; Wang, Y.; Wu, M. Antibiotic resistance gene abundances
614 associated with antibiotics and heavy metals in animal manures and agricultural soils adjacent
615 to feedlots in Shanghai; China. Journal of hazardous materials. 235:178-185; 2012
616 Kim, K.-H.; Kabir, E.; Jahan, S.A. A review on the distribution of Hg in the environment and its
617 human health impacts. Journal of hazardous materials. 306:376-385; 2016
618 Knapp, C.W.; McCluskey, S.M.; Singh, B.K.; Campbell, C.D.; Hudson, G.; Graham, D.W. Antibiotic
619 resistance gene abundances correlate with metal and geochemical conditions in archived
620 Scottish soils. PloS one. 6:e27300; 2011
621 Koczura, R.; Mokracka, J.; Taraszewska, A.; Łopacinska, N. Abundance of class 1 integron-integrase
622 and sulfonamide resistance genes in river water and sediment is affected by anthropogenic
623 pressure and environmental factors. Microbial ecology. 72:909-916; 2016
624 Lane, D.J. 16S/23S rRNA sequencing. in: Stackebrandt E., Goodfellow M., eds. Nucleic acid
625 techniques in bacterial systematics. New York, NY: John Wiley and Sons; 1991

626 Li, B.; Yang, Y.; Ma, L.; Ju, F.; Guo, F.; Tiedje, J.M.; Zhang, T. Metagenomic and network analysis
627 reveal wide distribution and co-occurrence of environmental antibiotic resistance genes. The
628 ISME journal. 9:2490; 2015
629 Lohren, H.; Blagojevic, L.; Fitkau, R.; Ebert, F.; Schildknecht, S.; Leist, M.; Schwerdtle, T. Toxicity
630 of organic and inorganic mercury species in differentiated human neurons and human
631 astrocytes. Journal of Trace Elements in Medicine and Biology. 32:200-208; 2015
632 Mahbub, K.R.; Bahar, M.M.; Megharaj, M.; Labbate, M. Are the existing guideline values adequate
633 to protect soil health from inorganic mercury contamination? Environment international.
634 117:10-15; 2018
635 Mahbub, K.R.; Krishnan, K.; Megharaj, M.; Naidu, R. Mercury inhibits soil enzyme activity in a
636 lower concentration than the guideline value. Bulletin of environmental contamination and
637 toxicology. 96:76-82; 2016a
638 Mahbub, K.R.; Krishnan, K.; Naidu, R.; Andrews, S.; Megharaj, M. Mercury toxicity to terrestrial
639 biota. Ecological Indicators. 74:451-462; 2017a
640 Mahbub, K.R.; Krishnan, K.; Naidu, R.; Megharaj, M. Mercury toxicity to *Eisenia fetida* in three
641 different soils. Environmental Science and Pollution Research. 24:1261-1269; 2017b
642 Mahbub, K.R.; Subashchandrabose, S.R.; Krishnan, K.; Naidu, R.; Megharaj, M. Mercury alters the
643 bacterial community structure and diversity in soil even at concentrations lower than the
644 guideline values. Appl Microbiol Biotechnol. 101:2163-2175; 2016b
645 Mahbub, K.R.; Subashchandrabose, S.R.; Krishnan, K.; Naidu, R.; Megharaj, M. Mercury alters the
646 bacterial community structure and diversity in soil even at concentrations lower than the
647 guideline values. Appl Microbiol Biotechnol. 101:2163-2175; 2017c
648 Mathema, V.B.; Thakuri, B.C.; Sillanpää, M. Bacterial mer operon-mediated detoxification of
649 mercurial compounds: a short review. Archives of microbiology. 193:837-844; 2011
650 Miller, W.; Miller, D. A micro-pipette method for soil mechanical analysis. Communications in Soil
651 Science & Plant Analysis. 18:1-15; 1987
652 Müller, A.K.; Westergaard, K.; Christensen, S.; Sørensen, S.J. The effect of long-term mercury
653 pollution on the soil microbial community. FEMS microbiology ecology. 36:11-19; 2001
654 Mulligan, C.N.; Yong, R.N. Natural attenuation of contaminated soils. Environment international.
655 30:587-601; 2004
656 Richards, R.; Taylor, R.; Zhu, Z. Mechanism for synergism between sulphonamides and trimethoprim
657 clarified. Journal of pharmacy and pharmacology. 48:981-984; 1996
658 Rosser, S.J.; Young, H.-K. Identification and characterization of class 1 integrons in bacteria from an
659 aquatic environment. Journal of Antimicrobial Chemotherapy. 44:11-18; 1999
660 Singer, A.C.; Shaw, H.; Rhodes, V.; Hart, A. Review of antimicrobial resistance in the environment
661 and its relevance to environmental regulators. Frontiers in microbiology. 7:1728; 2016
662 Száková, J.; Havlíčková, J.; Šípková, A.; Gabriel, J.; Švec, K.; Baldrian, P.; Sysalová, J.; Coufalík, P.;
663 Červenka, R.; Zvěřina, O. Effects of the soil microbial community on mobile proportions and
664 speciation of mercury (Hg) in contaminated soil. Journal of Environmental Science and
665 Health, Part A. 51:364-370; 2016
666 Turner, S.; Pryer, K.M.; Miao, V.P.; Palmer, J.D. Investigating deep phylogenetic relationships
667 among cyanobacteria and plastids by small subunit rRNA sequence analysis. The Journal of
668 eukaryotic microbiology. 46:327-338; 1999
669 Vikesland, P.J.; Pruden, A.; Alvarez, P.J.; Aga, D.; Bürgmann, H.; Li, X.-d.; Manaia, C.M.; Nambi, I.;
670 Wigginton, K.; Zhang, T. Toward a comprehensive strategy to mitigate dissemination of
671 environmental sources of antibiotic resistance. ACS Publications; 2017
672 Wardwell, L.H.; Jude, B.A.; Moody, J.P.; Olcerst, A.I.; Gyure, R.A.; Nelson, R.E.; Fekete, F.A. Co-
673 selection of mercury and antibiotic resistance in sphagnum core samples dating back 2000
674 years. Geomicrobiology Journal. 26:238-247; 2009
675 Wireman, J.; Liebert, C.A.; Smith, T.; Summers, A.O. Association of mercury resistance with
676 antibiotic resistance in the gram-negative fecal bacteria of primates. Appl Environ Microbiol.
677 63:4494-4503; 1997
678 Yang, C.-l.; Sun, T.-h.; He, W.-x.; Zhou, Q.-x.; Su, C. Single and joint effects of pesticides and
679 mercury on soil urease. Journal of Environmental Sciences. 19:210-216; 2007

680 Zhou, Y.; Niu, L.; Zhu, S.; Lu, H.; Liu, W. Occurrence, abundance, and distribution of sulfonamide
681 and tetracycline resistance genes in agricultural soils across China. Science of The Total
682 Environment. 599:1977-1983; 2017
683 Zhu, W.; Li, Z.; Li, P.; Yu, B.; Lin, C.-J.; Sommar, J.; Feng, X. Re-emission of legacy mercury from
684 soil adjacent to closed point sources of Hg emission. Environmental pollution. 242:718-727;
685 2018

686